MAX-PLANCK-INSTITUT
FÜR PLASMAPHYSIK

Electron temperature gradient control experiments in W7-X and the simulated response of electron- and ion-scale turbulence

Wendelstein 7-X

G.M. Weir, J.H.E. Proll, P. Xanthopoulos, A. Zocco, M. Hirsch, T. Stange, S. Stroteich, O. Grulke, G. Fuchert, N.A. Pablant, A. Langenberg, L. Podavini, H.M. Smith, S. Bozhenkov, E. Pasch, T. Klinger and the W7-X Team

Paper rehearsal, W7-X Physics Meeting
Sep. 1st, 2025, Greifswald, Germany

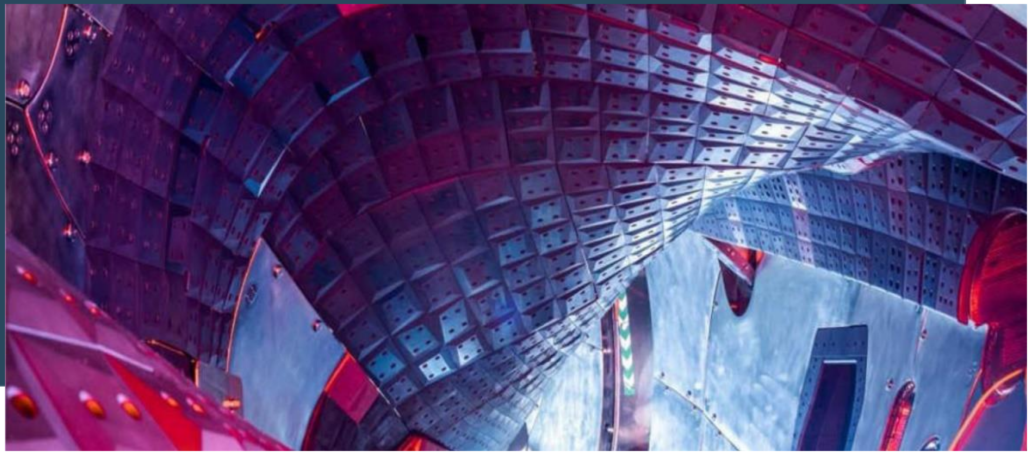

EUROfusion

This work has been carried out within the framework of the EUROfusion Consortium, funded by the European Union via the Euratom Research and Training Programme (Grant Agreement No 101052200 — EUROfusion). Views and opinions expressed are however those of the author(s) only and do not necessarily reflect those of the European Union or the European Commission. Neither the European Union nor the European Commission can be held responsible for them.

Abstract

Electron temperature gradient control experiments with concurrent Electron Cyclotron Resonance Heating (ECRH) power modulation have been performed in the “standard” magnetic configuration of W7-X in which the drives for electron- and ion-scale turbulence were approximately equal ($T_e \approx T_i$ and $a/L_{Te} \approx a/L_{Ti}$). In these experiments, a tight coupling of the species was maintained across a limited radial range of the plasma ($0.3 \leq r/a \leq 0.5$).

The electron heat flux determined from the propagation of heat pulses across this region is measured to scale linearly with the electron temperature gradient with a low degree of stiffness ($\chi^{hp} \approx \chi_e$) that is consistent with previous results on W7-X. This low stiffness indicates no measurable T_e profile resiliency, although the turbulent electron heat flux driven by ∇T_e can be experimentally significant.

Comparison to nonlinear gyrokinetic simulations indicate that transport driven at the ion-scales by mixed Ion Temperature Gradient (ITG) and ∇T-Trapped Electron Mode (TEM) turbulence compares favorably to the experimental level in both magnitude and scaling.

Additionally, the simulated electron heat flux driven at the electron-scales by Electron Temperature Gradient (ETG) mode turbulence is approximately 10% of the experimental level, and thus ETG-driven transport can be considered benign in W7-X in scenarios with equal temperatures and sufficiently large ∇T -TEM/ITG turbulence levels.

Temperature gradient control experiments on W7-X:

- Varying ratio of ECRH power deposited across r/a=0.4
- Goal: to vary ∇T_e, while maintaining T_e≈constant
- Concurrent ECRH modulation of innermost source for heat pulse prop.

20-30% total ECRH power, 17 Hz, 67% duty cycle

[G.M. Weir, *et. al.* Nucl. Fusion 5 (2021)]

- Methodology developed at AUG and applied to AUG/DIII-D data

[F. Ryter, *et. al.* Nucl. Fusion 43 (2003)/J.C. Deboo, *et. al.* Phys. Plasmas 5 (2010)]

- First attempt on W7-X in OP1.2b: XP:20180821.21-23

→ ΔT_e ≈100 eV; T_e/T_i=1.0±0.1; a/L_{ne}=0.7±0.1;

while a/L_{Te} varied by factor of ~4

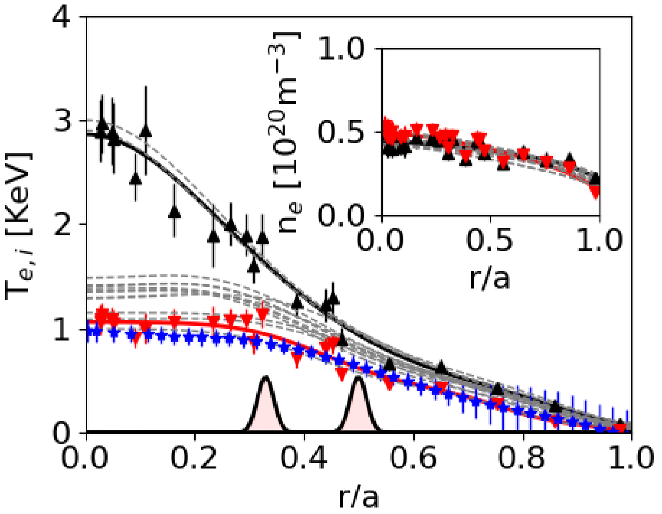

FIG. 1: Kinetic profiles measured during electron temperature gradient control experiments on W7-X. An on-axis (black △) and an off-axis (red ▽) heating case are highlighted, while profile fits are shown for intermediate experiments (grey lines). The ion temperature profile for the off-axis heating case is also shown (blue ▽). Plasma density profiles are inset. ECRH deposition regions are indicated by the shaded bell-curves at r/a=(0.3,0.5).Data from W7-X discharges XP:20180821.021-023.

Temperature gradient control experiments on W7-X:

- Tracking heat pulses generated by innermost ECRH source across this surface allows a direct measurement of the electron heat flux:

$$\chi_e^{HP} = -\frac{\partial(q_e/n_e)}{\partial \nabla T_e} \quad \rightarrow \quad \frac{q_e}{n_e} = -\int_0 \chi_e^{HP} d(\nabla T_e).$$

[J.C. Hillesheim, *et al.* PRL 43 (2013)]

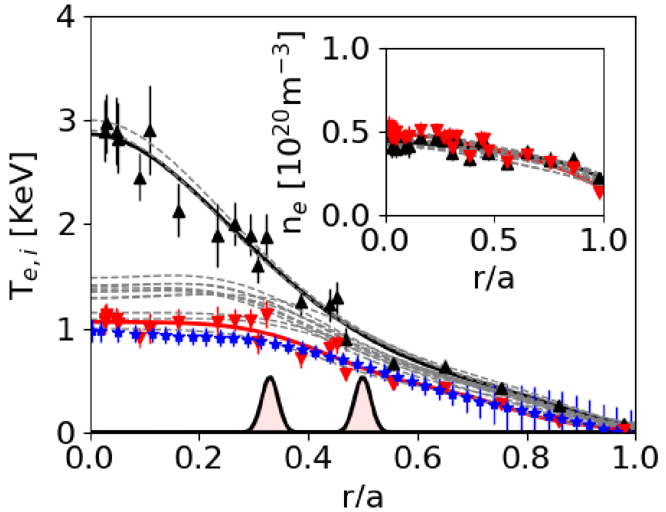

FIG. 1: Kinetic profiles measured during electron temperature gradient control experiments on W7-X. An on-axis (black △) and an off-axis (red ▽) heating case are highlighted, while profile fits are shown for intermediate experiments (grey lines). The ion temperature profile for the off-axis heating case is also shown (blue ▽). Plasma density profiles are inset. ECRH deposition regions are indicated by the shaded bell-curves at r/a=(0.3,0.5).Data from W7-X discharges XP:20180821.021-023.

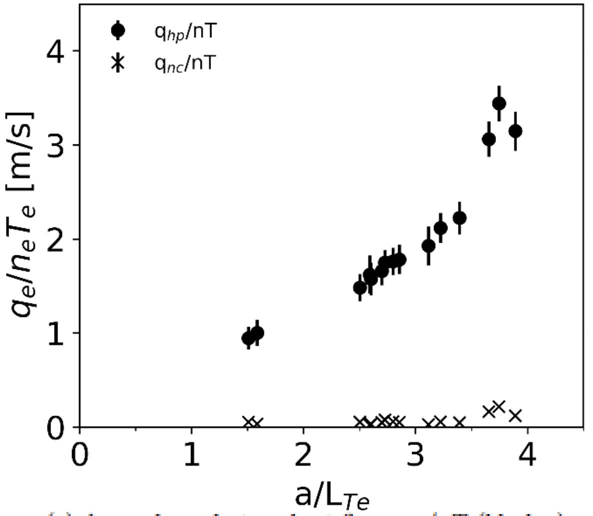

(a) Anomalous electron heat flux, q_{hp}/nT (black •), and neoclassical electron heat flux, q_{nc}/nT (black ×).

FIG. 2: The scaling of (a) the electron heat flux and (b) the electron thermal diffusivity derived from heat pulse propagation data against normalized electron temperature gradient.

Temperature gradient control experiments on W7-X:

- Tracking heat pulses generated by innermost ECRH source across this surface allows a direct measurement of the electron heat flux:

$$\chi_e^{HP} = -\frac{\partial(q_e/n_e)}{\partial \nabla T_e} \quad \rightarrow \quad \frac{q_e}{n_e} = -\int_0 \chi_e^{HP} d(\nabla T_e).$$

[J.C. Hillesheim, *et al.* PRL 43 (2013)]

→ Additional goal in these experiments on W7-X: $a/L_{Te} \approx a/L_{Ti}$ and $T_e \approx T_i$

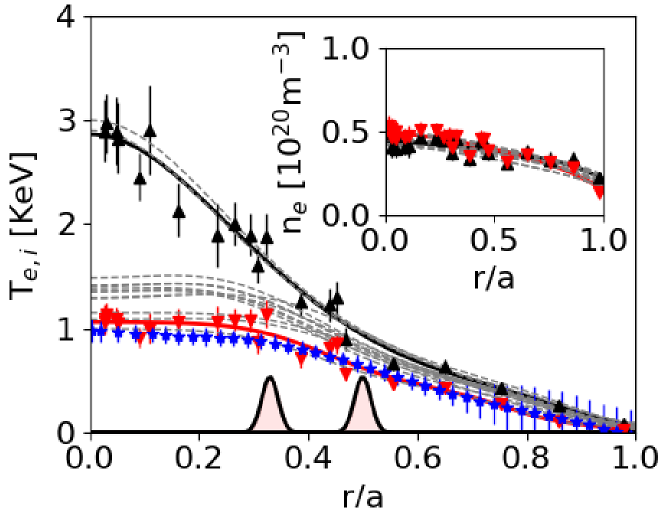

FIG. 1: Kinetic profiles measured during electron temperature gradient control experiments on W7-X. An on-axis (black △) and an off-axis (red ▽) heating case are highlighted, while profile fits are shown for intermediate experiments (grey lines). The ion temperature profile for the off-axis heating case is also shown (blue ▽). Plasma density profiles are inset. ECRH deposition regions are indicated by the shaded bell-curves at r/a=(0.3,0.5).Data from W7-X discharges XP:20180821.021-023.

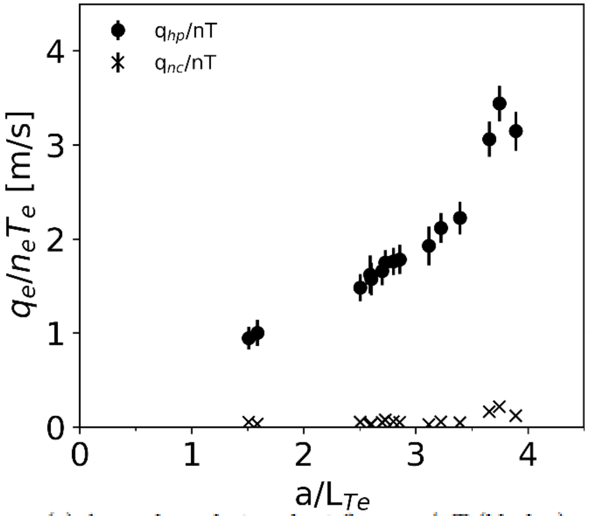

(a) Anomalous electron heat flux, q_{hp}/nT (black •), and neoclassical electron heat flux, q_{nc}/nT (black ×).

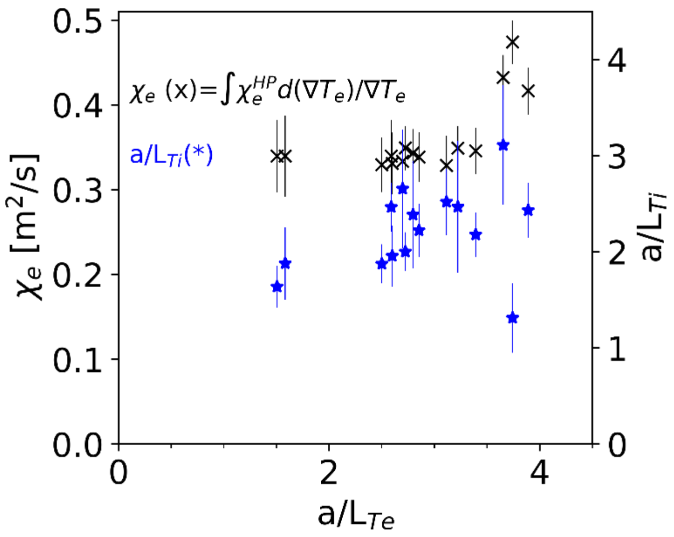

(b) Effective electron thermal diffusivity (black ×), and ion temperature gradient scale lengths (blue ∗).

FIG. 2: The scaling of (a) the electron heat flux and (b) the electron thermal diffusivity derived from heat pulse propagation data against normalized electron temperature gradient.

Temperature gradient control experiments on W7-X:

- Tracking heat pulses generated by innermost ECRH source across this surface allows a direct measurement of the electron heat flux:

$$\chi_e^{HP} = -\frac{\partial(q_e/n_e)}{\partial \nabla T_e} \quad \rightarrow \quad \frac{q_e}{n_e} = -\int_0 \chi_e^{HP} d(\nabla T_e).$$

[J.C. Hillesheim, *et al.* PRL 43 (2013)]

→ Additional goal in these experiments on W7-X: $a/L_{Te} \approx a/L_{Ti}$ and $T_e \approx T_i$

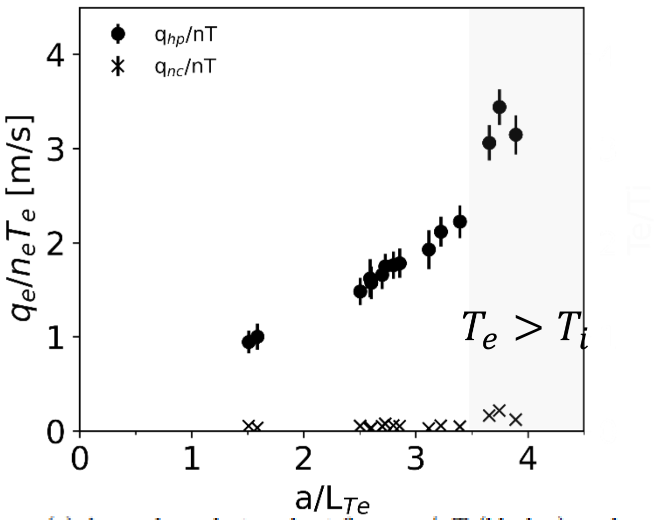

(a) Anomalous electron heat flux, q_{hp}/nT (black •), and neoclassical electron heat flux, q_{nc}/nT (black ×).

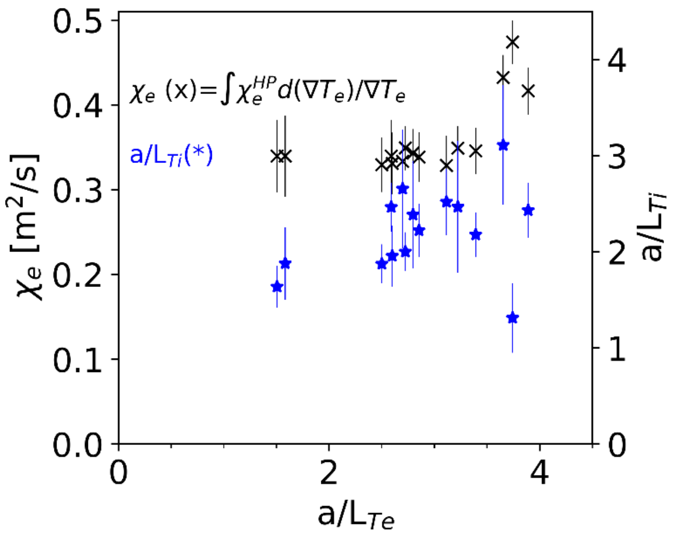

(b) Effective electron thermal diffusivity (black ×), and ion temperature gradient scale lengths (blue ∗).

q_e/n_e and χ_e can be determined independent from any modeling

$$\chi_e^{HP} \approx \chi_e$$

Consistent with results presented in G.M. Weir, *et. al.* Nucl. Fusion 5 (2021)

$T_e \approx T_i$,

$a/L_{Te} \approx a/L_{Ti}$,

for $a/L_{Te} \leq 3.7$

Above $a/L_{Te} > 3.7$ in these experiments corresponds with on-axis heating, $T_e > T_i$

FIG. 2: The scaling of (a) the electron heat flux and (b) the electron thermal diffusivity derived from heat pulse propagation data against normalized electron temperature gradient.

The simulated response of electron- and ion-scale turbulence

Nonlinear, collisionless flux-tube simulations at r/a=0.4 including both kinetic species:

→ Separated ion- and electron-scale simulations of the ITG/∇T-TEM (/UI) and ETG driven transport matching exp. w/ GX and STELLA as in [A. Zocco, *et. al.* PRR (2024)]

→ Separated ion- and electron-scale simulations of the ITG (a/L_{Te}=0) and ETG (a/L_{Ti}=0) driven transport that otherwise match exp. with GENE

→ Ion-scale simulations of the ∇T-TEM/ITG and ∇n-TEM/ITG where the magn. mirror-ratio, a/L_n and minor-radius (r/a) were varied with GX

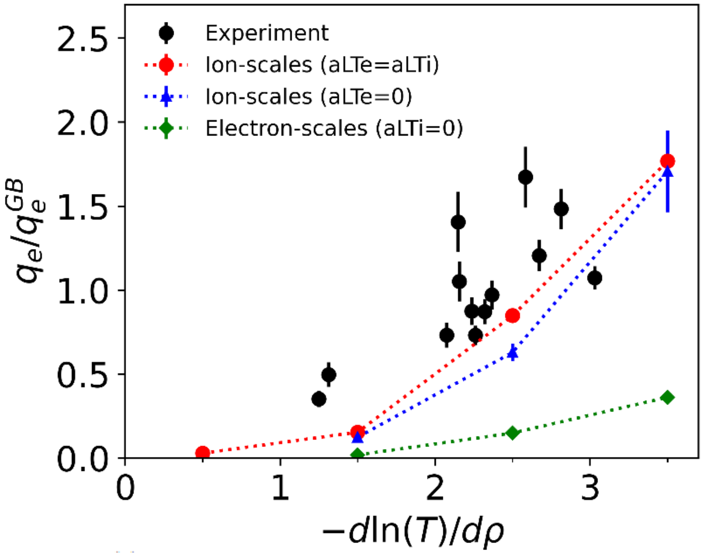

(a) Matching experimental parameters: ion-scale mixed ∇T-TEM/ITG (red circles) and ITG (blue triangles), and electron-scale ETG (green squares) simulations compared to experimental data (black circles)

FIG. 3: Gyro-Bohm normalized electron heat fluxes from simulation and experiment.

Ion-scale transport driven by the mixed ITG/∇T-TEM mode is dominant

Nonlinear, collisionless flux-tube simulations at r/a=0.4 including both kinetic species:

→ Separated ion- and electron-scale simulations of the ITG/∇T-TEM (/UI) and ETG driven transport matching exp. w/ GX and STELLA as in [A. Zocco, *et. al.* PRR (2024)]

→ Separated ion- and electron-scale simulations of the ITG (a/L_{Te}=0) and ETG (a/L_{Ti}=0) driven transport that otherwise match exp. with GENE

→ Ion-scale simulations of the ∇T-TEM/ITG and ∇n-TEM/ITG where the magn. mirror-ratio, a/L_n and minor-radius (r/a) were varied with GX

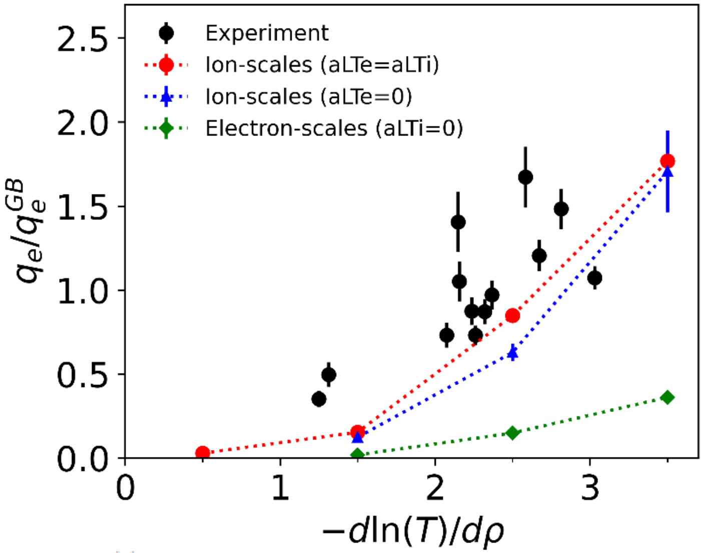

(a) Matching experimental parameters: ion-scale mixed ∇T-TEM/ITG (red circles) and ITG (blue triangles), and electron-scale ETG (green squares) simulations compared to experimental data (black circles)

Observations

1) Electron heat flux derived from ITG/∇T-TEM turbulence contributes more significantly to the total electron heat flux; ETG transport can matter

FIG. 3: Gyro-Bohm normalized electron heat fluxes from simulation and experiment.

ITG-only simulations drastically over-predict the ion heat transport (a/L_{Te}=0)

Nonlinear, collisionless flux-tube simulations at r/a=0.4 including both kinetic species:

→ Separated ion- and electron-scale simulations of the ITG/∇T-TEM (/UI) and ETG driven transport matching exp. w/ GX and STELLA as in [A. Zocco, *et. al.* PRR (2024)]

→ Separated ion- and electron-scale simulations of the ITG (a/L_{Te}=0) and ETG (a/L_{Ti}=0) driven transport that otherwise match exp. with GENE

→ Ion-scale simulations of the ∇T-TEM/ITG and ∇n-TEM/ITG where the magn. mirror-ratio, a/L_n and minor-radius (r/a) were varied with GX

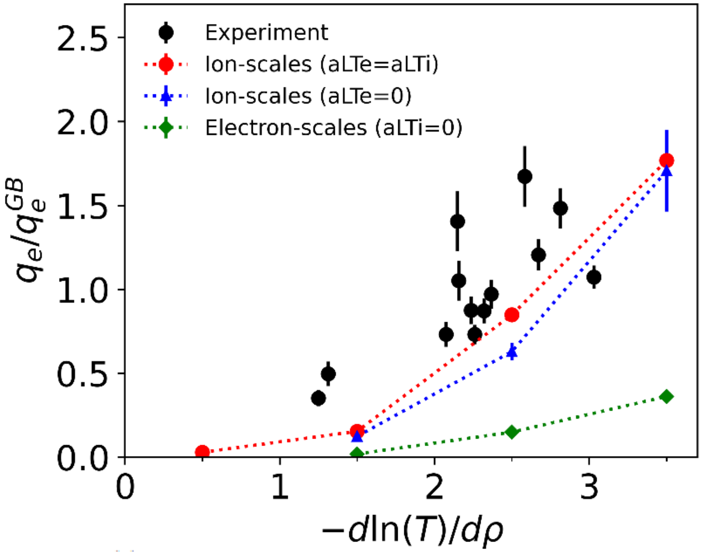

(a) Matching experimental parameters: ion-scale mixed ∇T-TEM/ITG (red circles) and ITG (blue triangles), and electron-scale ETG (green squares) simulations compared to experimental data (black circles)

<u>Observations</u>

1) Electron heat flux derived from ITG/∇T-TEM turbulence contributes more significantly to the total electron heat flux; ETG transport can matter
2) ITG (a/L_{Te}=0) only simulations appear okay, but the drastically over-predict the ion heat transport (~x20)

TABLE I: Ratio of total electron energy flux to convective energy flux ($Q_e/(5/2\Gamma T)$).

a/L_T	1.75	2.25	2.75
"pure" ITG:	0.98	0.99	0.95
∇T-TEM/ITG:	11.0	27.0	-135

FIG. 3: Gyro-Bohm normalized electron heat fluxes from simulation and experiment.

Quantitative and qualitative agreement with electron heat transport where $T_e \approx T_i$ and $a/L_{Te} \approx a/L_{Ti}$ for the ITG/∇T-TEM

Nonlinear, collisionless flux-tube simulations at r/a=0.4 including both kinetic species:

→ Separated ion- and electron-scale simulations of the ITG/∇T-TEM (/UI) and ETG driven transport matching exp. w/ GX and STELLA as in [A. Zocco, *et. al.* PRR (2024)]

→ Separated ion- and electron-scale simulations of the ITG (a/L_{Te}=0) and ETG (a/L_{Ti}=0) driven transport that otherwise match exp. with GENE

→ Ion-scale simulations of the ∇T-TEM/ITG and ∇n-TEM/ITG where the magn. mirror-ratio, a/L_n and minor-radius (r/a) were varied with GX

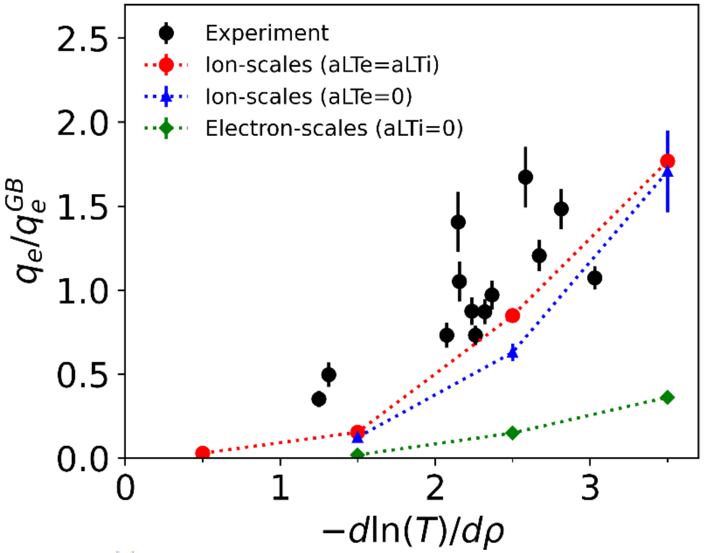

(a) Matching experimental parameters: ion-scale mixed ∇T-TEM/ITG (red circles) and ITG (blue triangles), and electron-scale ETG (green squares) simulations compared to experimental data (black circles)

TABLE I: Ratio of total electron energy flux to convective energy flux ($Q_e/(5/2\Gamma T)$).

a/L_T	1.75	2.25	2.75
"pure" ITG:	0.98	0.99	0.95
∇T-TEM/ITG:	11.0	27.0	-135

FIG. 3: Gyro-Bohm normalized electron heat fluxes from simulation and experiment.

<u>Observations</u>

1) Electron heat flux derived from ITG/∇T-TEM turbulence contributes more significantly to the total electron heat flux; ETG transport can matter
2) ITG (a/L_{Te}=0) only simulations appear okay, but the drastically over-predict the ion heat transport (~x20)
3) Quantitative and qualitative agreement with the electron heat transport in low-beta W7-X plasmas where $T_e \approx T_i$ and $a/L_{Te} \approx a/L_{Ti}$ for ITG/∇T-TEM driven turbulence

The most significant difference in configuration / parameter scans are the change with a/L_n between low- and high-mirror

Nonlinear, collisionless flux-tube simulations at r/a=0.4 including both kinetic species:

→ Separated ion- and electron-scale simulations of the ITG/∇T-TEM (/UI) and ETG driven transport matching exp. w/ GX and STELLA as in [A. Zocco, *et. al.* PRR (2024)]

→ Separated ion- and electron-scale simulations of the ITG (a/L_{Te}=0) and ETG (a/L_{Ti}=0) driven transport that otherwise match exp. with GENE

→ Ion-scale simulations of the ∇T-TEM/ITG and ∇n-TEM/ITG where the magn. mirror-ratio, a/L_n and minor-radius (r/a) were varied with GX

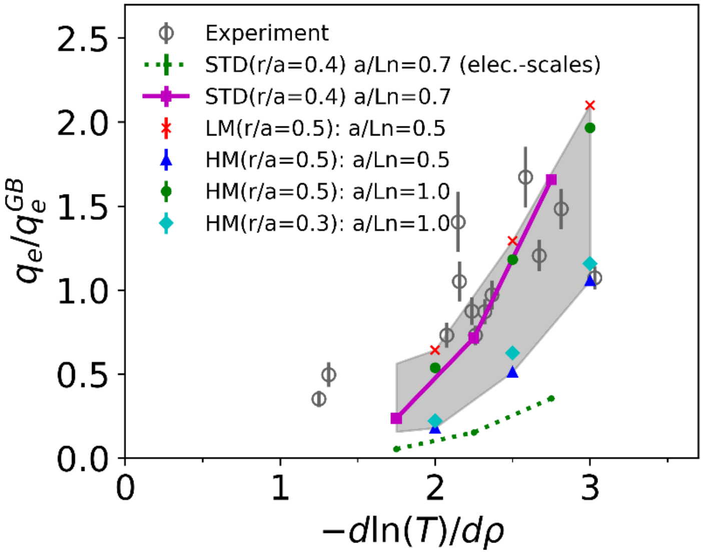

(b) "standard" (STD), "low-mirror" (LM), "high-mirror" (HM) ion-scale simulations and experimental data (grey circles) with varying mirror-ratio, a/L_n, and radial location in the extended configuration and parameter space of W7-X with $a/L_{Te} = a/L_{Ti}$ (electron-scale simulations specified). The convex hull of the simulated ion-scale data is shaded.

Observations

4) Greatest change in future experiments (performed in OP2) expected between low-mirror and high-mirror

→ High-mirror requires twice the density gradient driven to match low-mirror

FIG. 3: Gyro-Bohm normalized electron heat fluxes from simulation and experiment.

Summary and conclusions

∇T_e-control experiments in W7-X allow independent and direct measurements of the electron heat flux, Q_e

→ Tightly coupled species in region of interest: approximately equal drive for electron- and ion-scale turbulence $T_e \approx T_i$, $a/L_{Te} \approx a/L_{Ti}$

→ No critical gradient observed, and low-stiffness measured $\chi_e^{HP} \approx \chi_e$

→ Consistent with previous W7-X results [G.M.Weir, *et. al.* Nucl. Fusion 5 (2021)] and ITG-dominant scenarios on tokamaks [F. Ryter, et. al. PRL 95 (2005)]

Experimental measurements compare favorably to nonlinear gyrokinetic simulations of the mixed ITG/∇T-TEM transport:

→ Quantitative and qualitative agreement where $T_e \approx T_i$ and $a/L_{Te} \approx a/L_{Ti}$

→ Here, the electron transport does not grow explosively with a/L_{Te}, and the electron-scale contribution is ~10% of the experimental level